Regular and chaotic motions in applied dynamics of a rigid body

V. V. Beletskiĭ
M. V. Keldysh Institute of Applied Mathematics, 4 Miusskaya Sq., Moscow, 125047, Russia

M. L. Pivovarov
Space Research Institute, 84/32 Profsoyuznaya, Moscow, 117810, Russia

E. L. Starostin
M. V. Keldysh Institute of Applied Mathematics, 4 Miusskaya Sq., Moscow, 125047, Russia

(Received 25 February 1995; accepted for publication 1 March 1996)

Periodic and regular motions, having a predictable functioning mode, play an important role in many problems of dynamics. The achievements of mathematics and mechanics (beginning with Poincaré) have made it possible to establish that such motion modes, generally speaking, are local and form ''islands'' of regularity in a ''chaotic sea'' of essentially unpredictable trajectories. The development of computer techniques together with theoretical investigations makes it possible to study the global structure of the phase space of many problems having applied significance. A review of a number of such problems, considered by the authors in the past four or five years, is given in this paper. These include orientation and rotation problems of artificial and natural celestial bodies and the problem of controlling the motion of a locomotion robot. The structure of phase space is investigated for these problems. The phase trajectories of the motion are constructed by a numerical implementation of the Poincaré point map method. Distinctions are made between regular (or resonance), quasiregular (or conditionally periodic), and chaotic trajectories. The evolution of the phase picture as the parameters are varied is investigated. A large number of ''phase portraits'' gives a notion of the arrangement and size of the stability islands in the ''sea'' of chaotic motions, about the appearance and disappearance of these islands as the parameters are varied, etc. © *1996 American Institute of Physics.* [S1054-1500(96)00702-1]

I. DYNAMICS OF BODY OF TWO-LEGGED APPARATUS

One of the problems of controlling robotic devices is the problem of developing and testing mathematical models of walking devices, including two-legged. The following model, among others, was proposed and developed in Refs. 1–3. The two-dimensional problem of two-legged walking was considered. The two-legged apparatus was modeled by a rigid body equipped with a pair of two-member weightless legs. The walking consists only of single-support phases (only one leg provides support at any instant of time) and the legs make a point contact with the surface. Control moments in the knee and thigh of the supporting leg are used only to produce uniform and rectilinear horizontal motion of the suspension point of the legs. Through the action of a moment in the knee defined in this manner the heavy body of the apparatus can perform various motions. What are these motions?

The periodic motions of a body have been investigated in a number of papers,[4,5] sometimes together with motions similar to these. However, a global analysis of the phase trajectories of the problem is of considerable interest. The first results in this respect were obtained in Refs. 6–8 and are presented below.

The motion is investigated on the phase plane by means of a numerical implementation of the Poincaré point map method. Regular and chaotic motions are identified and their evolution is traced as parameters are varied. It is found, in particular, that stable periodic oscillations of the body with a center of mass that is located below the suspension point (''head down'') evolve to a stable periodic oscillation of the body, with the center of mass located above the suspension point (''head up'') as a parameter is varied. Chaotic motion of the body is typical and the periodic and conditionally periodic motions form ''islands'' in the chaotic ''sea.''

Figure 1 depicts schematically the two-legged device being investigated; it is shown at the moment when the supports are changing (from the ''back'' leg to the ''front''). We assume that J is the moment of inertia of the body (the body weight $P=Mg$) with respect to its center of mass, ρ is the distance from the center of mass to the suspension point of the legs, L is the length of a step, S is the ''support shift''—the distance of the projection of the suspension point of the legs on the support surface from the support point. We will assume that as the apparatus moves over a horizontal surface, the suspension point of the legs moves at a constant height h uniformly and rectilinearly with velocity V. (The moments of the control forces are easily expressed in terms of the reaction force of the support by virtue of the weightlessness of the legs.) We use the symbol ϑ to denote the inclination of the ''suspension point—center of mass'' axis to the axis directed vertically upward.

We define the dimensionless time τ in terms of the dimensioned time t by

$$d\tau=\omega\, dt, \quad \omega=\left(\frac{Mg\rho}{J+M\rho(\rho+h)}\right)^{1/2}. \tag{1}$$

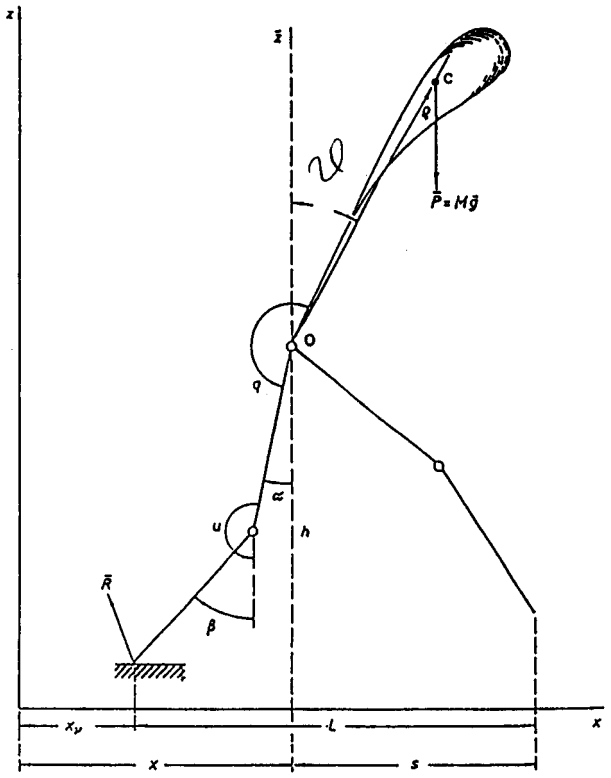

FIG. 1. A scheme of the two-legged device under study, shown at the moment of changing its supports from the ''back'' leg to the ''front.''

The dimensionless step duration $\tau_0=\gamma T$, where $T=L/V$, is the dimensioned stepping period. We introduce the other dimensionless parameters,

$$\lambda=L/\varrho, \quad \alpha=S/L, \quad \mu_1=M\varrho^2/[J+M\varrho(\varrho+h)],$$
$$\mu_2=\mu_1 h/\varrho, \tag{2}$$

and we assume

$$\varphi(\tau)=\tau/\tau_0-[\tau/\tau_0]-\alpha, \tag{3}$$

where $[z]$ denotes the integer part of z.

In these notations the equation of the body oscillations is:[1–3]

$$(1-\mu_2\cos\vartheta+\mu_1\lambda\varphi(\tau)\sin\vartheta)\frac{d^2\vartheta}{d\tau^2}$$
$$+[\mu_1\lambda\varphi(\tau)\cos\vartheta-\mu_2\sin\vartheta]\left(\frac{d\vartheta}{d\tau}\right)^2-\sin\vartheta=\lambda\varphi(\tau). \tag{4}$$

Equation (4) is nonlinear and non-Hamiltonian with periodic discontinuous coefficients. It has been investigated by many authors (see, for example, Refs. 3–5 and the bibliographies in these papers). These investigations, as already pointed out, were directed primarily at looking for periodic solutions of Eq. (4) and investigating their properties. The discontinuity of the coefficients of Eq. (4) with time is caused by the discontinuity of the single-support walking process. Equation (4) can be written in the form

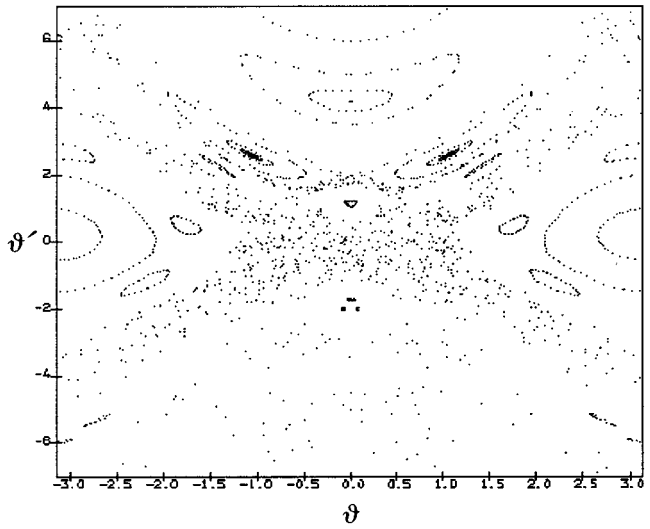

FIG. 2. The Poincaré map for $\lambda=1$, corresponding to the short step.

$$\frac{d^2\vartheta}{d\tau^2}-\sin\vartheta=q. \tag{5}$$

The operator on the left side of Eq. (5) is a result of the natural presence of a reversible pendulum in the problem while the function $q=q(\vartheta,d\vartheta/d\tau,\tau)$ expresses the control moment at the suspension point of this pendulum, which provides for a given translational motion (the Vukobratovich pre-defined synergy method[9]). Equation (4) is a five-parameter equation. In the calculations below it is assumed that $\mu_1=0.1$ and $\mu_2=0.3$. If no values are stated for α and τ_0, then it is assumed that $\alpha=0.5$ and $\tau_0=1.0$. Let us point out that for $\alpha\neq0.5$ the pattern of motion (or the phase portrait) differs qualitatively from the $\alpha=0.5$ case. The parameter λ is the principal variable parameter; it varies from figure to figure. Only the principal islands within a reasonable interval of the angular velocity, plotted along the ordinate axis, are identified in all of the figures cited below. The angle ϑ (in radians) of the deviation of the body from the vertically upright direction is plotted along the abscissa axis. The point maps are drawn for the period τ_0 of the duration of one walking step.

A typical Poincaré phase picture is depicted in Fig. 2. Here $\lambda=1$, which corresponds to the short step. There are many islands of regularity in the chaotic sea. The center of the main island of regularity ($\vartheta=\pm\pi$, $\vartheta'\sim0.1$) corresponds to stable periodic ''head-down'' motion with a one-step period. In the vicinity of this island there is an archipelago of five islands whose centers represent stable head-down motion with a period of five steps. The large island with the center ($\vartheta=0$, $\vartheta'\approx4$) corresponds to regular motions in the vicinity of a stable periodic forward rotation of the body with a period of one step. (Biological two-legged systems do not have such motions, but robot systems may not impose any restriction on body rotation.) Stable forward rotations of the body with a period of three steps are also seen. The remnants of destroyed islands near periodic reverse rotations with a period of three steps are visible in the lower part of the figure in the chaotic sea. Such rotations exist and are stable at smaller λ values.

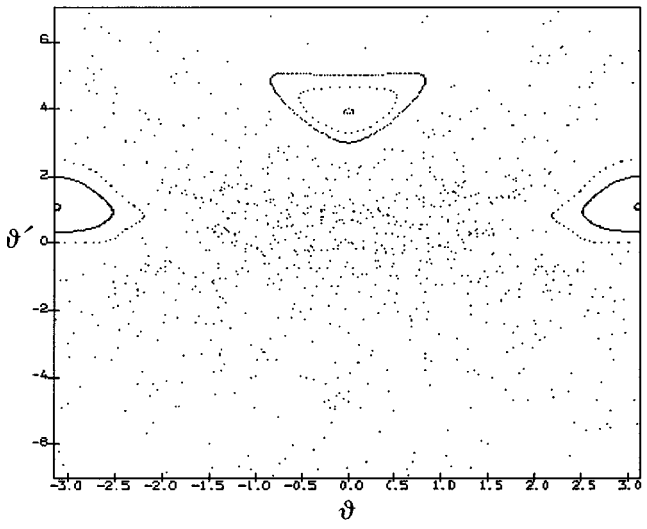

FIG. 3. The Poincaré map for an increased step length of $\lambda=5$.

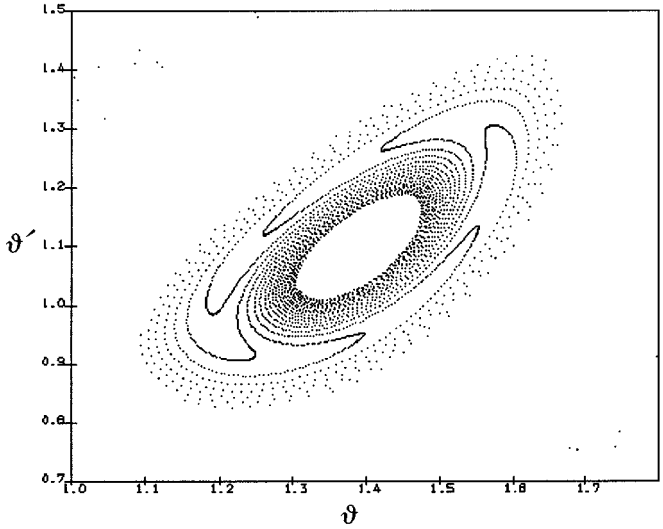

FIG. 5. The structure of the attractor at a magnified scale.

The phase picture shows that pendulum oscillation effects dominate near the bottom equilibrium position. The rotational motions are arranged nonsymmetrically: forward rotations along the path of the apparatus are more likely to be regular while reverse rotations are primarily chaotic.

Figure 3 illustrates the situation for an increased step length of $\lambda=5$. Two islands of regularity are clearly visible in the sea of chaos: ''head-down'' oscillations and regular forward rotations, in particular, a stable periodic rotation (center of the island). Bifurcation occurs with a further increase of λ: the island of stable oscillations is broken up into two. The center of the right island—periodic ''head-down—forward'' motion—is asymptotically stable within some attraction region (or attractor). The center of the left island—periodic ''head-down—backward'' motion—is unstable (or repeller).

With an increase in λ the repeller and attractor converge (Fig. 4, $\lambda=9$) and the periodic ''head-up—forward'' motion corresponds to motion for which the forward inclination is severe and the body is oriented nearly horizontally (the ''position of a skater''[4]). The structure of this attractor is depicted at a magnified scale in Fig. 5, where the point map of one trajectory is shown.

The subsequent evolution of the phase picture with an increase in λ passes through a change in stability ($\lambda\approx9.18$) when both the ''head-up—forward'' and ''head-up—backward'' motions are neutrally stable, and a stage when the repeller and attractor change positions. Then for $\lambda\approx11$ the repeller and attractor merge into one neutrally stable ''head-up'' motion (Fig. 6). With a further increase of λ existence is preserved and the periodic ''head-up'' motion with a period of the duration of one step continues to remain neutrally stable. (Attendant stable periodic oscillations with a period of several steps can appear.)

Some conclusion about stability can be drawn by examining the variation equation with respect to the solutions of

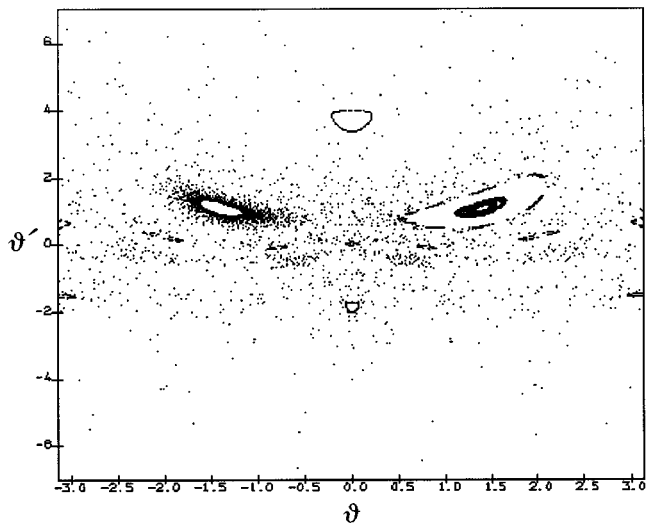

FIG. 4. The repeller and attractor converge as λ increases.

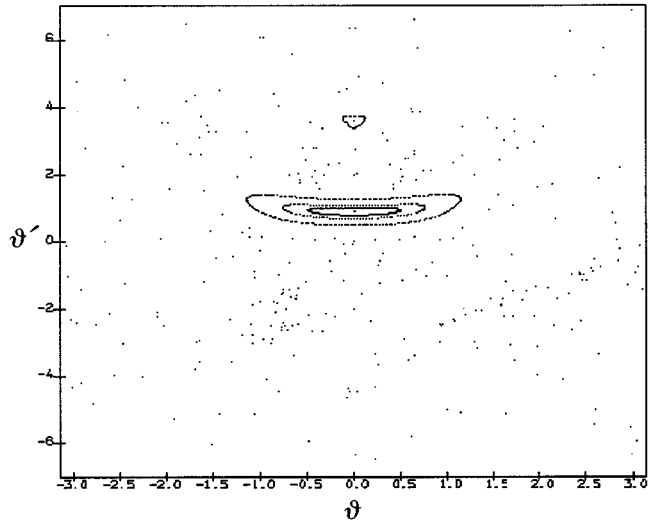

FIG. 6. For $\lambda\approx11$ the repeller and attractor merge into one neutrally stable ''head-up'' motion.

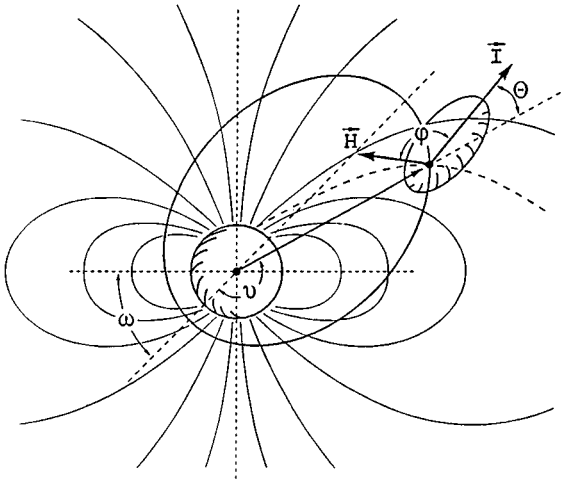

FIG. 7. A satellite in an elliptic polar orbit in the gravitational and magnetic fields of the Earth.

Eq. (4). Thus, in the case of a periodic oscillation of the body in the vicinity of $\vartheta=0$ the variation equation in a reasonable approximation has the form

$$\frac{d^2(\delta\vartheta)}{d\tau^2}+(\mu_1\lambda^2\varphi^2-1)(\delta\vartheta)=0. \tag{6}$$

For $\alpha=0.5$ the average value $(1/\tau_0)\int_0^{\tau_0}\varphi^2 d\tau = 1/12$. Therefore, the condition

$$\mu_1\lambda^2>12 \tag{7}$$

can be considered as the estimated stability condition of periodic motion in the vicinity of $\vartheta\approx 0$. For the value of $\mu_1=0.1$ being used this is equivalent to the condition $\lambda>11$, and this is what is observed (Fig. 6).

Thus far phase portraits of the problem have been considered for $\alpha=0.5$. A deviation of α from this value alters the phase portrait qualitatively.

The wealth of possibilities existing as the parameters are varied is remarkable. Thus, for $\lambda=9$ and $\alpha=0.49$ all three basic regular motions (single-periodic forward rotation and single-periodic ''head-forward'' and ''head-back'' oscillations) are asymptotically stable so that three regular attractors appear in the chaotic sea. For $\lambda=9$ and $\alpha=0.51$, however, three repellers are obtained conversely: all three regular motions are unstable (compare with the case $\lambda=9$, $\alpha=0.5$ in Fig. 4).

II. SATELLITE IN ORBIT. GRAVITATIONAL, MAGNETIC, AND TIDAL MOMENTS

Figure 7 depicts a satellite in an elliptic polar orbit in the gravity and magnetic field of the Earth. The moment of the gravitational gradient forces and the moment of the magnetic forces from the interaction of the Earth's magnetic field with a permanent, by assumption, magnet mounted on the satellite act on the satellite. Both of these moments are potential (and the equations of motion can be given in Hamiltonian form). We also take dissipative forces into account by using the formal construction of the tidal moment to do this. This approach is used for investigation of the rotation of natural celestial bodies, but in the case of artificial celestial bodies it will make it possible to determine the trends and qualitative features of the influence of dissipative factors.

Taking into consideration the aforesaid, equation of two-dimensional motions of the satellite, in the plane of the polar orbit, with respect to the center of mass can be written as

$$(1+e\cos\nu)\frac{d^2\theta}{d\nu^2}+[\beta(1+e\cos\nu)^5-2e\sin\nu]\frac{d\theta}{d\nu}$$
$$+\frac{n^2}{2}\sin 2\theta+\frac{\alpha}{2}[\cos(\theta+u)-3\cos(\theta-u)]=2e\sin\nu;$$
$$u=\nu+\omega. \tag{8}$$

Here ν is the true anomaly and is an independent variable, ω is the constant inclination of the radius vector of the perigee of the satellite orbit with respect to the Earth's equator, e is the eccentricity of the orbit, $n^2=3(A-C)/B$ is the gravitational parameter corresponding to the moment of the gravitational forces; A,B,C are the principal central moments of inertia of the satellite; $\alpha=I\mu_E/B\mu$ is the magnetic parameter, corresponding to the moment of the magnetic forces; the magnetic field is assumed to be that of a dipole with the magnetic moment μ_E whose axis coincides with the Earth's axis; and μ is the gravitational constant. The satellite rotates about the axis corresponding to the moment of inertia B; this axis is normal to the plane of the orbit. The constant magnetic moment I of the satellite is directed along the axis corresponding to the moment of inertia C; this axis forms the angle θ with the running radius vector of the orbit. The moment of the dissipative forces is determined by the term with the dissipation coefficient β; as already stated, the structure of this moment is chosen to coincide with the structure of the moment of the tidal forces.

The quantities $n^2,\alpha,e,\omega,\beta$ emerge in the role of parameters of the problem. The parameter ω has no significance since varying it does not alter the qualitative structure of the phase portrait. The statement that the orbit being considered is polar refers only to the $\alpha\neq 0$ case (a magnetic moment is present). If $\alpha=0$, then Eq. (8) is valid, of course, for an orbit with any inclination.

The following special cases of Eq. (8), which are of greatest interest, will be considered.

(1) $\alpha=\beta=0$, $n^2\neq 0$, $e\neq 0$. The satellite (or any celestial body) is revolving in an elliptic orbit due to the action of the gravitational gradient forces. The equation for this special case was first obtained in Ref. 10:

$$\delta=2\theta;\ (1+e\cos\nu)\frac{d^2\delta}{d\nu^2}-2e\sin\nu\frac{d\delta}{d\nu}+n^2\sin\delta=4e\sin\nu. \tag{9}$$

(2) $\alpha=0$, $\beta\neq 0$, $n^2\neq 0$, $e\neq 0$. The preceding case is supplemented by the action of the moment of tidal forces. The equation in this form is of special interest for explaining the capture of natural celestial bodies in resonance rota-

tion modes. The role of the tidal moment for this situation was considered, for example, in Ref. 11.

(3) $\beta=n^2=e=0$, $\alpha\neq 0$. The satellite is revolving in a circular polar orbit acted on by only the moment of magnetic forces. Equation (8) for this case was first introduced in Ref. 12 in the variables u and φ, where φ is the deviation angle of the satellite axis from the magnetic line of force. Equation (8) in these variables is transformed to the following:

$$\frac{d^2\varphi}{du^2}+\alpha(\sqrt{1+3\sin^2 u})\sin\varphi=6\frac{\sin 2u}{(1+3\sin^2 u)^2}. \quad (10)$$

(4) $\beta=0$, $n^2\neq 0$, $\alpha\neq 0$. $e\neq 0$. The satellite is revolving in a polar elliptic orbit in the gravitational and magnetic field. The equation in this case was obtained in Ref. 13. The case of a circular orbit: $e=0$, $\beta=0$, $n^2\neq 0$, $\alpha\neq 0$, is of special interest here.

Equation (8) in the above-stated special forms of (1)–(4) has been investigated by many authors—primarily for the existence and stability of regular (or periodic) motions—especially for Eqs. (9) and (10). Information about these investigations can be found in books and reviews such as Refs. 11, 12, 14–18. However, there have been few investigations of the global structure of phase space, its rearrangement as the parameters are varied, and the relations of the regular and chaotic motions. Among investigations in this area let us point out Refs. 19–22. The possibility of the chaotic motion of Hyperion was demonstrated in Ref. 19 within the framework of the problem (1); the chaotic and regular motions in this problem were examined in Ref. 20 for several values of the parameters; the appearance of chaos via period doubling bifurcation was traced in Ref. 21 within the framework of this same problem for the solutions of Eq. (9); the structure of the phase space of Eq. (10) was investigated in Ref. 22.

The results of a global analysis of the phase trajectories of Eq. (8) in the special forms of (1)–(4) are described below. Some of these results are contained in the preprint[23] while some are being described for the first time. Phase portraits of Eq. (8) on the ϑ,ϑ' plane are given for different parameter values. It is assumed that $\omega=0$, unless otherwise stated. The phase portraits were calculated by a numerical implementation of the Poincaré point map method. The period of the point map coincides with the orbital period. A reasonable calculation region, corresponding to moderate angular velocities, is chosen on the phase portraits. This region contains modes of motion that are of interest from the viewpoint of a practical implementation for artificial satellites (orientation along the radius vector, along a magnetic line of force, etc.). On the other hand, this region also corresponds to the greatest chaotization of motion. (By virtue of the finiteness of the force moments it is quite obvious that the motion is regular for sufficiently large angular velocities.)

The accuracy with which the ''regularity islands'' are isolated in the ''sea of chaos'' was determined by the same considerations of common sense and practical expediency; islands that were too small were generally not isolated.

Figure 8 shows a typical phase picture of Eq. (9) or,

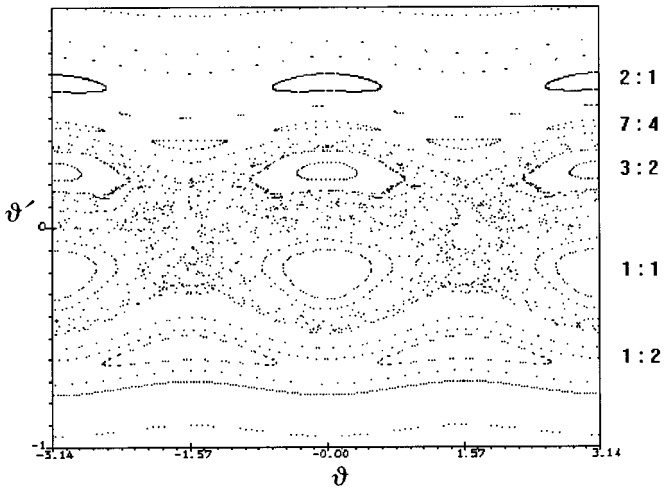

FIG. 8. The Poincaré map of Eq. (9) for $e=0.1$ and $n^2=0.1$. No magnetic and dissipative moments.

what is the same thing, Eq. (8) for $\alpha=\beta=0$. The following parameter values were chosen: $e=0.1$ and $n^2=0.1$. In other words, magnetic and dissipative moments are absent, a gravitational moment exists, and the orbit is elliptic. The inertia ellipsoid does not differ from a sphere ($n^2=0$) by very much. A series of ''islands'' in a ''sea'' of chaos is observed, as usual. The centers of the islands correspond to stable motions:

$$\theta=\frac{k-m}{m}\nu+\kappa(\nu);\quad \kappa(\nu+2\pi m')=\kappa(\nu), \quad (11)$$

where k,m,m' are pairwise coprime integers. We will call such motion a $k{:}m$ resonance. Here k denotes the number of revolutions (in absolute space) that the satellite performs about its own axis during m orbital revolutions. The type of resonance for each ''archipelago'' is indicated in the figure. The 1:1 resonance—''Earth orientation'' (similar to the Moon)—represents periodic oscillations about the running radius vector; the 3:2 resonance represents a rotation like that of Mercury; the 2:1 resonance represents orientation with respect to the magnetic line of force.

The stability of this last resonance is noteworthy. It is natural to achieve magnetic orientation by means of a magnet mounted on the satellite. As seen from Fig. 8, however, one can even bypass this and achieve magnetic orientation purely by means of the gravitational moment, ensuring, in particular, the existence and stability of the 2:1 resonance, among others. (However, adjustment of the magnet, of course, improves the quality of the magnetic orientation, increases the stability region, etc.)

We will now switch on the dissipative moment in order to follow the mechanism for locking in resonance motions. Point maps of the phase trajectories of Eq. (8) are depicted in Fig. 9 for $\alpha=\omega=0$, $e=0.1$, $n^2=0.1$, $\beta=0.002$. The trajectory is calculated in such a manner that it begins at a certain level of angular velocity ($\theta_0'=0.8$) and it continues until explicit capture in a given resonance; then the initial angular deviation θ_0 is changed (in small increments) and the calculation

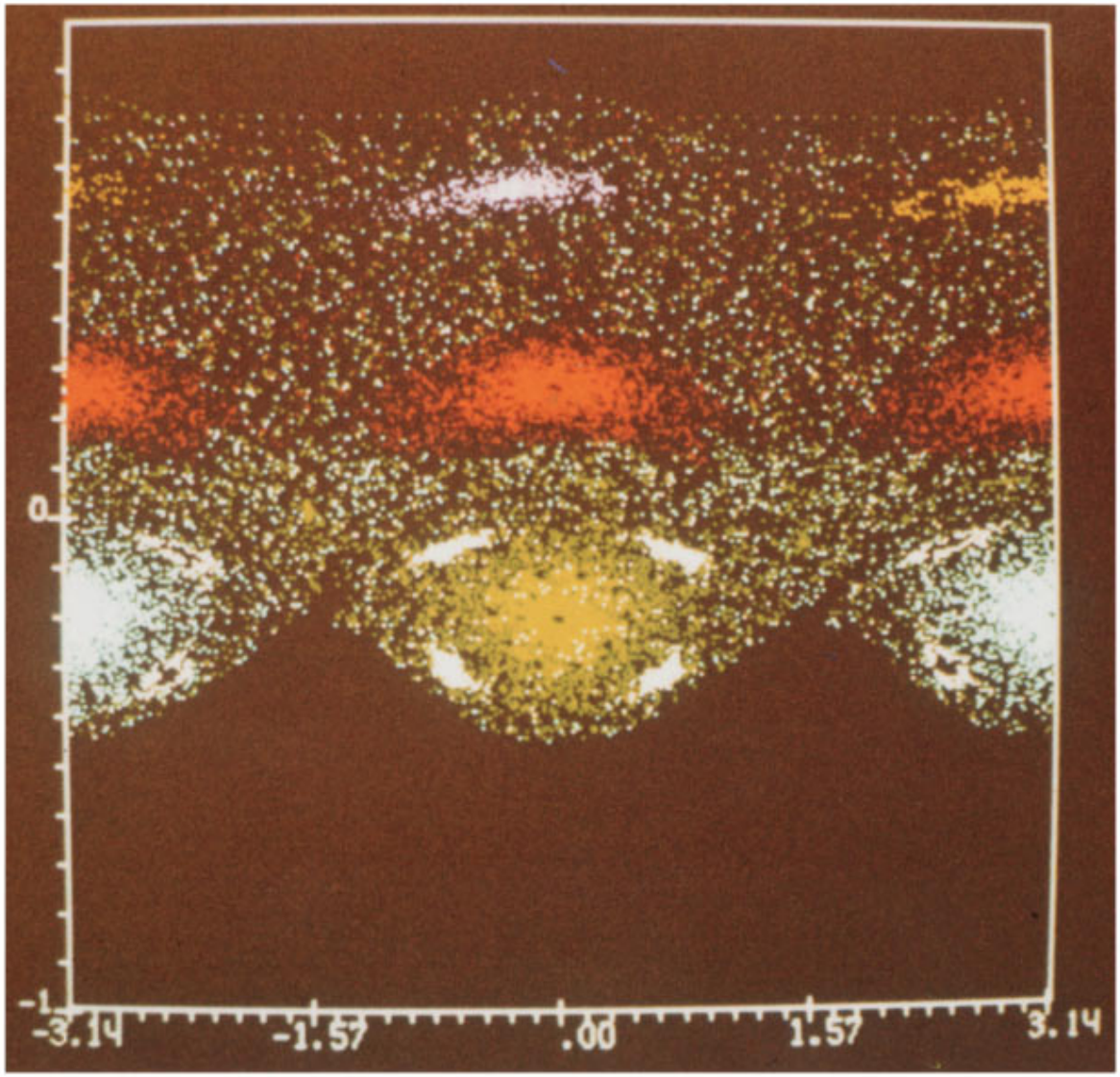

FIG. 9. Capture into resonant rotations under dissipation: $e=0.1$, $n^2=0.1$, $\beta=0.02$. The points on a trajectory captured by a certain resonance are colored in the same color. Blue and yellow—capture into 2:1 resonance (with different phases). Red—capture into 3:2 resonance. Green and sky blue—capture into 1:1 resonance (with different phases). Periodic oscillations of the orbital period are superimposed on all the above rotations. White—capture into 1:1 resonance. Periodic oscillations are superimposed, with the period four times larger than the orbital one.

of a new trajectory begins from the same level $\theta_0' = 0.8$, etc. Each limiting resonance mode corresponds to its own color, in which all of the trajectories attracted to this limiting mode are colored. The attraction of the trajectories to the 1:2 resonance, to the T-periodic 1:1 resonance, to the $4T$-periodic 1:1 resonance (T is the orbital period), and to the 3:2 and 2:1 resonances is traced on the figure.

It is known that dissipation coefficients β that are too large can lead to a ''smearing'' of the resonances: the trajectories are not captured in sufficiently high-order resonances. In our problem the capture condition in the k:2 resonance can be written as

$$\beta < \Phi_k(e)\,\frac{n^2}{|k-2|}, \tag{12}$$

where $\Phi_k(e)$ is a completely defined function of the arguments e and k (see, for example, Refs. 14 and 16). By using the $\Phi_k(e)$ expression for small e values, we obtain the following table of capture conditions for arbitrary values of e and n^2 (the third column of Table I) and specifically for $e=n^2=0.1$ (the fourth column of Table I).

For a value of $\beta=0.002$, for which the trajectories in Fig. 9 were calculated, capture must occur in all of the listed resonances. This is also observed in the figure. The results of a calculation of the fraction of the trajectories, captured in a given resonance in the numerical experiment for $e=n^2=0.1$ and two β values of 0.005 and 0.002, are shown in Table II.

TABLE I.

k	k:2	(12)	(12): $e=0.1$; $n^2=0.1$
1	1:2	$\beta<en^2/2$	$\beta<0.005$
2	1:1	$\beta<\infty$	$\beta<\infty$
3	3:2	$\beta<7en^2/2$	$\beta<0.035$
4	2:1	$\beta<17e^2n^2/4$	$\beta<0.004\,25$

TABLE II.

	k:2				
β	1:2	1:1	3:2	2:1	Σ
0.005	0.000	T:0.740 $4T$:0.125	0.135	0.000	1.000
0.002	0.060	T:0.680 $4T$:0.050	0.190	0.020	1.000

It is seen from Table II that for $\beta=0.005$ capture does not occur in the 1:2 and 2:1 resonances, just as should be the case according to theoretical estimates.

While there are no low-order stable resonances for $\beta=0$, a chaotic attractor is possible in principle for $\beta\neq 0$ as the limiting motion mode. Such a case is depicted in Fig. 10 ($\alpha=\omega=0$, $n^2=3$, $e=0.4$, $\beta=0.005$). For the 1:1 resonance the chosen parameter values give an instability because of parametric resonance. The $n^2=3$ value corresponds, for example, to a dumbbell-shaped satellite. The limiting mode (Fig. 10) has the well-known attributes of a chaotic attractor—fractal structure, etc. 5000 points are represented in Fig. 10.

Let us now turn to the (3) ($\beta=0$, $n^2=0$, $e=0$, $\alpha\neq 0$) and (4) ($\beta=0$, $e=0$, $n^2\neq 0$, $\alpha\neq 0$) cases, i.e., to the problem of magnetic and magnetic-gravitational interaction with the satellite.

Everywhere below we assume $\beta=0$. In Fig. 11(a) ($e=0$, $n^2=0$, $\alpha=0.05$, $\omega=0$) the case of a ''magnetic'' satellite in a circular orbit in the absence of a gravitational moment is considered. In this case stable orientation with respect to the magnetic field is observed (the 2:1 resonance)—similar to the orientation of a compass needle along a magnetic line of force. At the same time a large island, corresponding to the 0:1 resonance, is observed somewhat unexpectedly. The center of this island corresponds to a periodic motion that ensures, on the average, an orientation in absolute space parallel to the axis of the Earth's magnetic dipole.

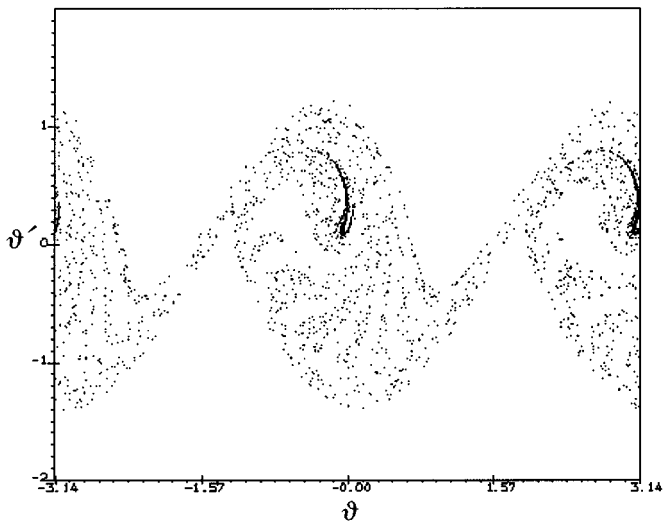

FIG. 10. The Poincaré map of Eq. (8) for $\alpha=\omega=0$, $\beta=0.005$, $e=0.4$, and $n^2=3$. Here 5000 points are represented.

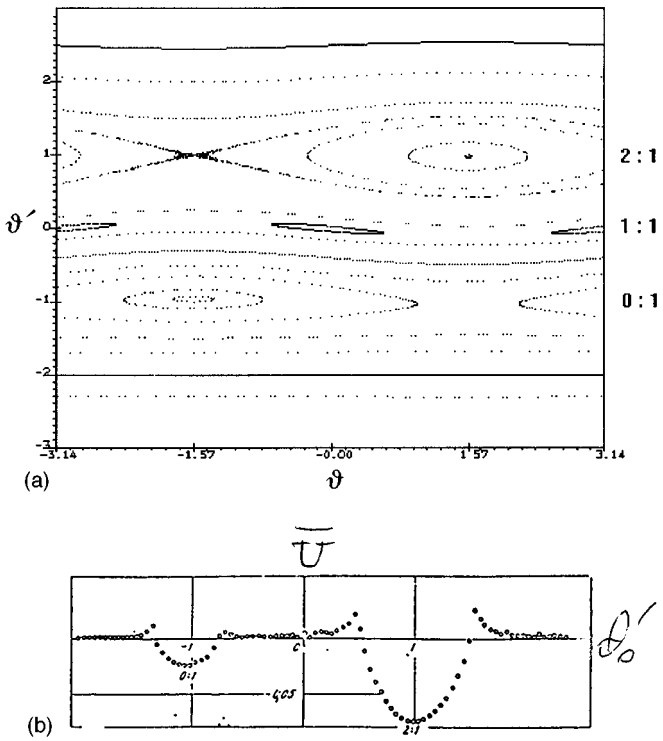

FIG. 11. (a) The Poincaré map of Eq. (8) for $\alpha=0.05$, $\omega=0$, $\beta=0$, $e=0$, and $n^2=0$. A ''magnetic'' satellite in a circular orbit in the absence of a gravitational moment. (b) The average potential of the acting moments for the case of (a).

The criterion for isolating the initial data θ_0, θ_0' for stable resonance motions was proposed and confirmed by a numerical experiment in Ref. 24: the points (θ_0,θ_0') must be the local minimum points of the average potential of the moments of the acting forces,

$$\overline{U}(\theta_0,\theta_0')=\lim_{t\to\infty}\frac{1}{t}\int_0^t U[\theta(\theta_0,\theta_0',t),\theta'(\theta_0,\theta_0',t),t]dt. \tag{13}$$

Here U is the potential of the moment of the acting forces.

A graph of Eq. (13) is shown in Fig. 11(b) for the case depicted in Fig. 11(a). Sharp minima are clearly seen for the 2:1 and 0:1 resonances.

At the same time, narrow islands of the 1:1 resonance are seen in Fig. 11(a). This means that the magnetic moment, in principle, can also provide for the orientation of the satellite along the radius vector without the action of a gravitational moment, but in this case the stability region is small. In Fig. 11(b) the corresponding local minimum is not visible for the calculation accuracy employed.

One could expect that switching on the gravitational moment in the situation shown in Fig. 11(a) will increase the 1:1 resonance region. This turned out to be true [Fig. 12(a):

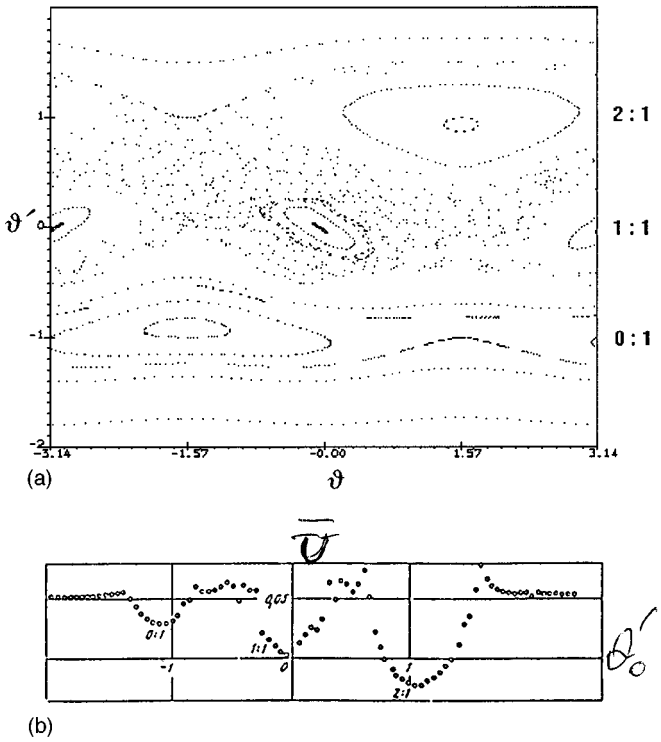

FIG. 12. (a) The Poincaré map of Eq. (8) for $\alpha=0.05$, $\omega=0$, $\beta=0$, $e=0$, and $n^2=0.2$. A satellite in a circular orbit under the influence of both the magnetic and gravitational moments. (b) The average potential of the acting moments for the case of (a).

$e=0$, $n^2=0.2$, $\alpha=0.05$]. Switch-on of the gravitational moment leads to an improvement of the conditions for orientation along the radius vector and to an enlargement of the regularity islands of the 1:1 resonance, but also to a chaotization of the motions in the vicinity of these islands. Figure 12(b) shows a graph of Eq. (13) for this case. It is seen from the figure that a new local minimum, corresponding to the 1:1 resonance, appears.

Different criteria of chaotic motion are well known in nonlinear dynamics.[25] At the same time, the criteria of motion regularity, such as criteria of the type (13), are also of interest.

Let us describe the evolution of the phase picture of the magnetic oscillations of a satellite ($e=0$, $n^2=0$) as the parameter α is varied. When the value of α is increased, the picture shown in Fig. 11(a) varies in the following manner: chaotization increases, and archipelagos of islands appear, whose centers correspond to long-period motions. Thus, 2π- and 8π-periodic oscillations are observed in Fig. 13 ($\alpha=0.2$). With a small increase of the parameter α the 8π-periodic oscillations vanish: the islands retreat into the sea and they drown in it. Bifurcation occurs for $\alpha\approx0.295$, and 6π-periodic oscillations are produced inside the 2:1 island (Fig. 14, $\alpha=0.3$). Then, this archipelago also disappears in the sea, etc. with an increase in α. The 10π-periodic oscillations produced in the vicinity of the 0:1 resonance are also visible in Fig. 15 ($\alpha=0.35$). A bifurcation of the principal 2:1 island into two islands occurs for $\alpha\approx0.6$. Increasing the parameter α does not contribute to stabilization in absolute space: the

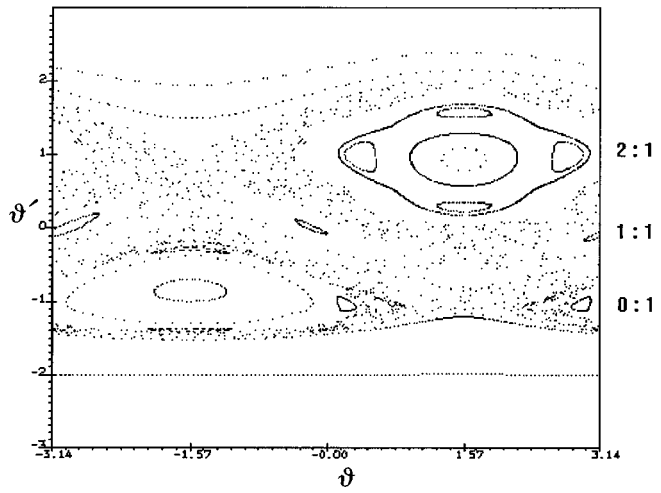

FIG. 13. The Poincaré map of Eq. (8) for $\alpha=0.2$, $\omega=0$, $\beta=0$, $e=0$, and $n^2=0$. A ''magnetic'' satellite in a circular orbit in the absence of a gravitational moment.

0:1 island decreases in size and vanishes forever for $\alpha>0.7$. The 2:1 island also vanishes for $\alpha\approx0.8$, and the motion becomes completely chaotic. Then the 2:1 island reappears and its subsequent bifurcation, vanishing and appearance occur in accordance with the theory of magnetic nonlinear 2π-periodic oscillations.[16,17]

To conclude this section let us give an example of the chaotic interaction of gravitational and magnetic oscillations in a circular orbit ($e=0$, $n^2=3$, $\alpha=1$). The gravitational and magnetic moments, separately, give either complete regularity ($e=0$, $n^2=3$, $\alpha=0$) or an island of regularity ($e=0$, $n^2=0$, $\alpha=1$), in combination, however, they give complete chaotization in the same portion of phase space.

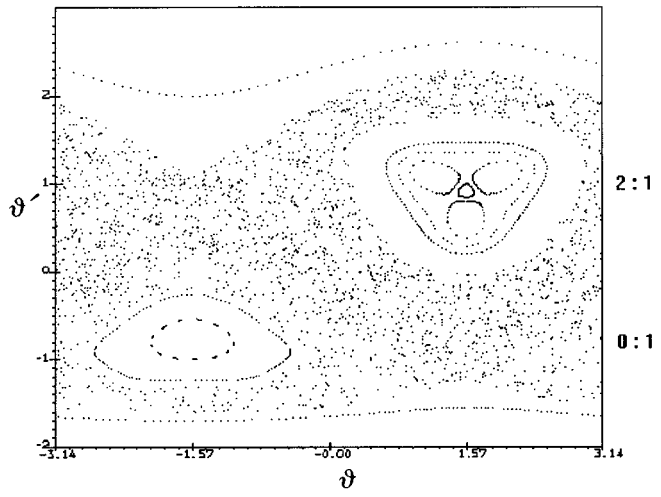

FIG. 14. The Poincaré map of Eq. (8) for $\alpha=0.3$, $\omega=0$, $\beta=0$, $e=0$, and $n^2=0$. A ''magnetic'' satellite in a circular orbit in the absence of a gravitational moment.

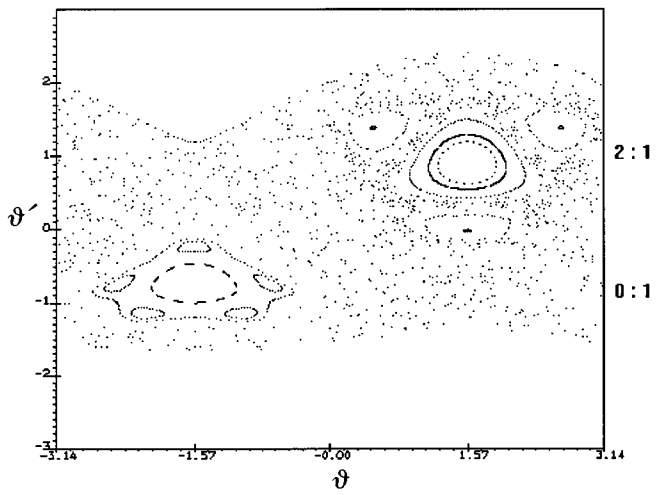

FIG. 15. The Poincaré map of Eq. (8) for $\alpha=0.35$, $\omega=0$, $\beta=0$, $e=0$, and $n^2=0$. A ''magnetic'' satellite in a circular orbit in the absence of a gravitational moment.

III. ROTATION OF CELESTIAL BODY IN GRAVITATIONAL FIELD OF TWO CENTERS

The model problem of the motion of a celestial body with respect to its center of mass due to the action of the gravitational moments from two attracting centers is considered. A point mass m moves along a Keplerian circular orbit of radius R in the gravity field of the point mass M (Fig. 16). The center of mass O of the rigid body K of finite size moves around M along a Keplerian circular orbit of radius $\rho<R$. The orientation of the body K with respect to the radius vector of its center of mass is described by the angle β, measured from this radius vector to one of the principal inertia axes of the body. All of the motion occurs in one plane and deviations of the trajectories from Keplerian circular trajectories are ignored. The mutual angular position of the center of mass O of the body K and the point m is described by the angle α; since $\rho<R$, $d\alpha/dt>0$.

Gravitational moments from the side of the attracting centers M and m act on the body K.

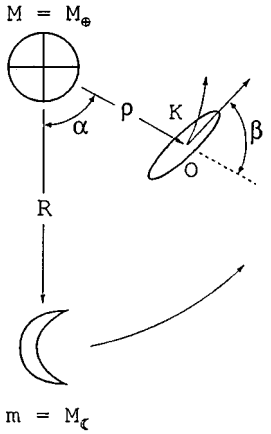

FIG. 16. Rotation of body K of finite size moving in gravitational field of two centers M and m.

The described model formulation will be specified for the Earth–artificial Earth satellite–Moon and Sun–Venus–Earth systems.

The motion of the body K with respect to its center of mass in this model formulation is described by

$$\frac{d^2\beta}{d\alpha^2}+\frac{n^2}{2}\left(\frac{1}{1-\lambda^{3/2}}\right)^2\sin 2\beta+\frac{n^2}{2}\left(\frac{\lambda^{3/2}}{1-\lambda^{3/2}}\right)\epsilon f(\alpha,\beta)=0, \tag{14}$$

where

$$f(\alpha,\beta)=\frac{\lambda^2\sin 2\beta-2\lambda\sin(2\beta+\alpha)+\sin(2\beta+2\alpha)}{(1+\lambda^2-2\lambda\cos\alpha)^{5/2}},$$

$$\epsilon=\frac{m}{M};\quad \lambda=\frac{\rho}{R};\quad n^2=3\frac{A-C}{B}, \tag{15}$$

and A,B,C are the principal central moments of inertia of the body K, with B being the moment of inertia with respect to the axis normal to the plane of the orbit and C being the moment of inertia with respect to the axis forming the angle β with the running radius vector (we assume for the sake of being specific that $B>A>C$).

We introduce into the discussion the deviation χ from the possible resonance rotation

$$\beta=p\alpha+\chi, \tag{16}$$

where p is a positive or negative half-integer (or, generally speaking, any rational number).

For $\epsilon=0$, Eq. (14) is the usual equation of rotation of a rigid body in a circular orbit in the gravity field of a point with mass M; the term with $\epsilon\neq 0$ describes perturbations due to the influence of the second center of mass m. These perturbations make it possible to expect that resonance modes (16) can appear with functions $\chi(\alpha)$ that are periodic with respect to α; in this case, as follows from Kolmogorov–Arnold–Moser (KAM) theory, the width of the resonance zone is

$$\Delta_r\sim\frac{n\lambda^{3/2}}{1-\lambda^{3/2}}\sqrt{\epsilon}\varphi(p), \tag{17}$$

and the width of the ''stochastic'' layer,[25] i.e., the chaotic motion region in the vicinity of a given resonance, is

$$\Delta_s\sim\exp\left(-\frac{1}{\Delta_r}\right). \tag{18}$$

Here $\varphi(p)<1$ is a function of the resonance number p.[26]

It follows from Eqs. (17) and (18) that the resonance and chaos effects increase (or decrease) with an increase (or decrease) in the parameters n,λ,ϵ.

Let us point out that the coefficients of Eq. (14) are 2π periodic with respect to the independent variable α; the values of $\alpha=2\pi k$, $k=0,1,2,...$, correspond to the inferior conjunctions of the point m and body K. If $\chi(\alpha)$ is 2π periodic with respect to α in Eq. (16), then resonances with the integers p correspond to those rotations of the body K for which in each inferior conjunction the same side of it is turned toward the m center.

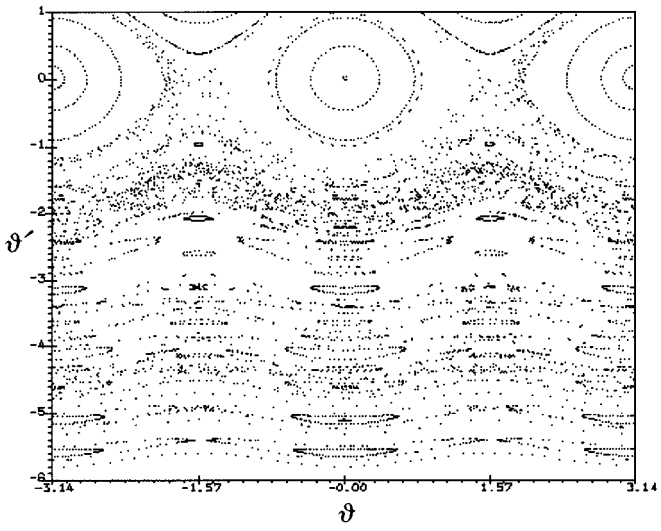

FIG. 17. The Poincaré map of the Earth–artificial Earth satellite–the Moon system for $\lambda=0.7$ and $n^2=0.3$.

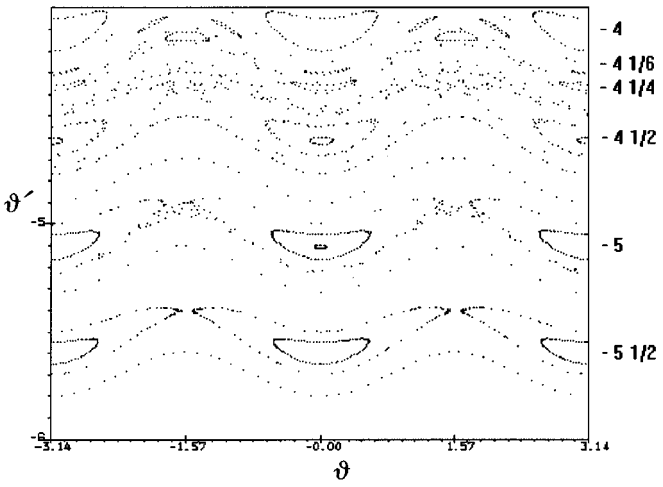

FIG. 18. Magnification of the region of retrograde motion in Fig. 17.

Let us consider a satellite in the terrestrial and lunar field. We then have M as the Earth's mass, m is the lunar mass, and K is an artificial Earth satellite. In this case $\epsilon=1/81.3\approx0.0123$. The upper limit of λ is determined from the condition that the orbit of the satellite in the Earth–Moon system is located completely outside the sphere of lunar activity. The model formulation being considered makes sense only in this case. Values of $\lambda<0.83$ satisfy this condition.

Figure 17 is a phase portrait of the problem (14) for $\lambda=0.7$ and $n^2=0.3$. In this case the perturbations are comparatively large because of the large λ value (the satellite periodically approaches close to the center m). The phase portrait is obtained by a numerical implementation of the Poincaré point map method with period 2π in terms of the independent variable α. The centers of the large regularity islands visible in this figure correspond to a stable periodic oscillation of the satellite about the running radius vector (a gravitational orientation of the satellite at Earth). In terms of Eq. (16) this means that $p=0$. Numerous regularity islands with $p\neq0$, located in the chaotic sea, are also visible. A characteristic feature of the phase portrait is the absence of symmetry with respect to the sign of the resonance parameter p. A resonance zone with $p=p_-<0$ is an order of magnitude wider than a zone with $p=p_+>0$, $p_+=|p_-|$. In other words, ''retrograde'' rotations of the satellite are perturbed more strongly than analogous direct rotations. The chaotic sea floods this region of retrograde rotations.

A fragment of the picture of Fig. 17 in the retrograde rotation region is shown in Fig. 18. Archipelagos, corresponding to resonances with a multiplicity of 1/2, 1/4, 1/6, are visible. The resonance in the vicinity of $\beta'=-5$ corresponds to the value of $p=-5$, and Venus rotates in the vicinity of such a resonance in the Sun–Venus–Earth system. The value of λ in this system is close to $\lambda=0.7$; therefore, the fragment depicted in Fig. 18 can be considered as a model of the ''Venus type'' and similar resonances; however, the value of ϵ in the Sun–Venus–Earth system is several orders of magnitude smaller than here. More details about the Venus rotation model will be given below.

Let us point out one of the results of a calculation of the phase portrait of the problem (14). A new feature is observed for $\lambda=0.7$ and $n^2=3$: two stable periodic oscillations of the satellite (and one unstable) with respect to the radius vector ($p=0$) exist rather than just one.

Let us now turn to the Venus rotation problem. Radar measurements carried out in the first half of the 1960s made it possible to determine that Venus rotates about its own axis, which is almost normal to the plane of its orbit, backward with respect to the orbital motion with a period of ≈243 Earth days. It was pointed out in Ref. 27 that the period is close to resonance motion (16) with $\chi(\alpha+2\pi)=\chi(\alpha)$ and with a value of $p=-5$. In this case the exact resonance period of rotation is equal to 243.16 days. This gave rise to a series of investigations of the Venus rotation phenomenon.[11,14,28,29] The extremely small width of the resonance zone and the extremely small probability of the capture of Venus in resonance rotation, as well as other obstacles to the realization of resonances, were pointed out, in particular.

According to present-day data,[30] the rotation period of Venus is equal to 243.022 ± 0.006 Earth days. The principal central moments of inertia A,B,C $(B>A>C)$ of Venus satisfy the ratios

$$\alpha=(B-A)/C=(8.52\pm0.51)10^{-6},$$

$$\beta=(B-C)/A=(16.71\pm0.51)10^{-6},$$

$$\gamma=(A-C)/B=(8.19\pm0.33)10^{-6}.$$

This means that the true rotation of Venus lies entirely outside the resonance zone, with the discrepancy between the angular velocity of Venus and the resonance value being an order of magnitude greater than the width of the resonance zone. Several papers[30–33] have pointed this out.

The calculation results presented below also confirm this fact.

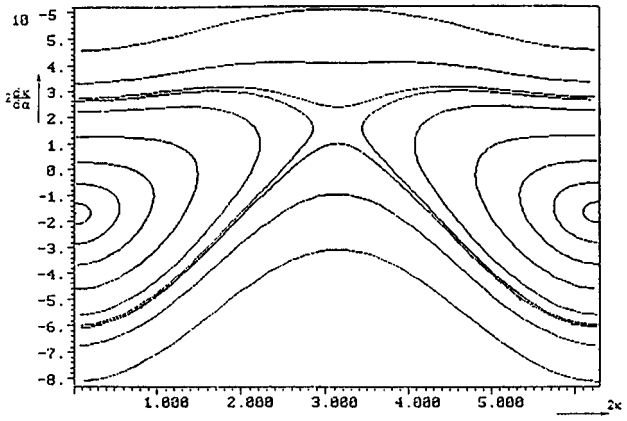

FIG. 19. Phase trajectories of the Sun–Venus–Earth system in the vicinity of the resonance $p=-5$. Here $\epsilon=3.004\times10^{-6}$, $\lambda=0.723\,332$, and $n^2=2.457\times10^{-5}$.

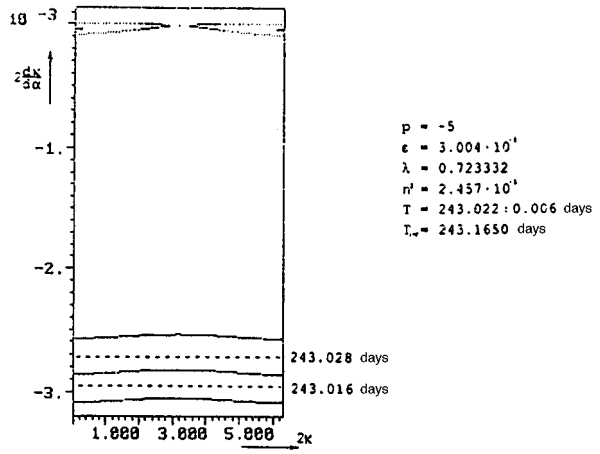

FIG. 20. The relative location of the resonance $p=-5$ zone and the observed rotation of Venus, according to modern data.

Let us consider Eq. (14) as the model description of the Venus rotation in the gravity field of the Sun (M) and Earth (m). Taking the data of Ref. 31 into account, we assume

$$\epsilon=3.004\times10^{-6},\quad \lambda=0.723\,332,\quad n^2=2.457\times10^{-5}.$$

These values correspond to the estimate of Eq. (17) $\Delta_r\sim10^{-5}$–10^{-6}. In view of Eq. (18), this denotes the essential absence of a stochastic layer; the smallness of the width of the resonance zone causes serious difficulties in calculating it. Figure 19 shows the cuts of KAM tori, calculated numerically, by the $(\chi,d\chi/d\alpha)$ plane in the vicinity of the resonance $p=-5$. In the region being considered the motion of the imaging point, corresponding to successive Poincaré maps, occurs very slowly along smooth curves. Tens of thousands of maps (from 20 000 to 100 000) must be calculated in order to plot one of the curves depicted in Fig. 19. Thus, two vastly different time scales are present in the problem: the period of the map and the time required for the imaging point to bypass the entire smooth curve. This means that such a problem is stiff. In order to speed up the computational process a special two-stage method was developed. In essence it consists of the fact that the numerical construction of the smooth curves on the secant plane is carried out on the basis of information about the vector field supplied by means of a numerical construction of several successive Poincaré maps at the required points of the plane.

As seen from Fig. 19, the resonance tori are very flattened. In the vicinity of those points of the curves where the tangent is parallel to the ordinate axis, the cross sections of the tori are constructed in the usual manner by means of successive iterations of the mapping. A program based on an extrapolation method was used to calculate the individual Poincaré maps.

Such a two-stage approach made it possible to reduce the required computational costs by two orders of magnitude compared with a direct integration for the same global error value.

Figure 20 shows the relative arrangement of the resonance zone being investigated and the $d\chi/d\alpha$ values, corresponding to modern data from observations of the proper Venus rotation period. The boundary of the interval of measured values of the quantity $d\chi/d\alpha$ is depicted by the dashed lines. As seen from the figure, the distance along the ordinate axis between the resonance zone and the observed values exceeds the width of the resonance zone by about an order of magnitude.

In conclusion, let us mention the following fact. Resonances with a multiplicity of $\frac{1}{2}$ correspond to the following rotation periods:

$$p=-4.5,\quad T=307.111\ \text{Earth days},$$
$$p=-5.0,\quad T=243.165\ \text{Earth days},$$
$$p=-5.5,\quad T=201.259\ \text{Earth days}.$$

Even though the true Venus rotation period (243.022 ± 0.006 Earth days), as shown, lies outside the resonance zone of the $p=-5.0$ resonance, it is clearly attracted to it, being spaced from the nearest resonances of the same multiplicity by a ''distance'' that is several orders of magnitude greater than the ''distance'' from the $p=5.0$ resonance.

This may or may not mean something. The question of the nature and origin of the retrograde rotation of Venus with the above-stated observed period remains unanswered.[34]

Note added in proof. Some of the results presented have been published as rather inaccessible preprints of the M. V. Keldysh Institute of Applied Mathematics, Russian Academy of Sciences,[6,23,35,36] as well as in Refs. 7, 8, 37, and 38. These publications do not overlap the material contained herein, nor does this review overlap the cited publications.

ACKNOWLEDGMENTS

The authors acknowledge with gratitude support of the Russian Foundation of Basic Research, through Grant No. 95-01-00308a.

[1] V. V. Beletskiĭ, ''Dynamics of two-legged walking,'' preprint No. 32, M. V. Keldysh Institute of Applied Mathematics, Academy of Sciences USSR, 1974.

[2] V. V. Beletskiĭ, ''Dynamics of two-legged walking I, Izv. Akad. Nauk SSSR; Mekh. Tverd. Tela No. 3 (1975); II, Izv. Akad. Nauk SSSR, Mekh. Tverd. Tela No. 4 (1975).
[3] V. V. Beletskiĭ, *Two-Legged Walking—Model Problems of Dynamics and Control* (Nauka, Moscow, 1984).
[4] E. K. Lavrovskiĭ, ''Dynamics of two-legged walking for large motion velocities,'' Izv. Akad. Nauk SSSR, Mekh. Tverd. Tela No. 4 (1980).
[5] V. V. Beletskiĭ and M. D. Golubitskaya, ''Stabilization and resonance effects in two-legged walking,'' Prikl. Mat. Mekh. No. 2 (1991).
[6] V. V. Beletskiĭ, ''Regular and chaotic motions of body of two-legged apparatus,'' preprint No. 52, M. V. Keldysh Institute of Applied Mathematics, Academy of Sciences USSR, 1990.
[7] V. V. Beletzky, ''Nonlinear effects in dynamics of controlled two-legged walking,'' in *Nonlinear Dynamics in Engineering Systems*, edited by W. Schiehlen (Springer-Verlag, Berlin, 1990).
[8] V. V. Beletzky, ''Regular and chaotic movements of body of two-legged apparatus,'' in *Lecture Notes of the ICB Seminars on Biomechanics*, edited by M. Dietrich (ICB, Warsaw, 1992).
[9] M. Vukobratovich, *Walking Robots and Anthropomorphic Mechanisms* (Mir, Moscow, 1976).
[10] V. V. Beletskiĭ, *On Satellite Libration, Colloquium: Artificial Earth Satellites* (Academy of Sciences, USSR, 1959), No. 3.
[11] P. Goldreich and S. Peale, ''The dynamics of planetary rotations,'' Annu. Rev. Astron. Astrophys. **6**, 287 (1968).
[12] V. V. Beletskiĭ, *Motion of Artificial Satellite with Respect to Center of Mass* (Nauka, Moscow, 1965).
[13] A. A. Khentov, ''Effect of magnetic and gravitational fields on oscillation of satellite about its center of mass,'' Kosmich. Issled. **5**, No. 4 (1967).
[14] V. V. Beletskiĭ, *Satellite Motion with Respect to Center of Mass in Gravitational Field* (University of Moscow Press, Moscow, 1975).
[15] V. A Sarychev, ''Questions of the orientation of artificial Earth satellites,'' *Summaries of Science and Engineering, Series: Space Research* (Viniti, Moscow, 1978).
[16] V. V. Beletskiĭ and A. A. Khentov, *Rotational Motion of Magnetized Satellite* (Nauka, Moscow, 1985).
[17] V. A. Sarychev and M. Yu. Ovchinnikov, ''Magnetic orientation systems of artificial Earth satellites,'' *Summaries of Science and Engineering, Series: Space Research* (Viniti, Moscow, 1985).
[18] V. V. Beletsky, ''Resonant phenomena in rotational motions of artificial and natural celestial bodies,'' in *Theoretical and Applied Mechanics*, edited by F. I. Niordson and N. Olhoff (North-Holland, New York, 1985).
[19] J. Wisdom, S. J. Peale, and F. Mignard, ''The chaotic rotation of Hyperion,'' Icarus **58**, 137 (1984).
[20] X. Tong and F. P. J. Rimrott, ''Numerical studies on chaotic planar motion of satellites in an elliptic orbit,'' Chaos, Solitons, Fractals **1**, No. 2 (1991).
[21] V. I. Gulyaev, A. L. Zubritskaya, and V. L. Koshkin, ''Universal sequence of period doubling bifurcations of the oscillations of a satellite in an elliptic orbit,'' Izv. Akad. Nauk SSSR, Mekh. Tverd. Tela No. 3 (1989).
[22] Z. S. Batalova and N. A. Mel'nichenko, ''On the structure of phase space and bifurcations of the equation of motion of a magnetized satellite in the plane of a circular polar orbit,'' Kosmich. Issled. **21**, 512 (1983).
[23] V. V. Beletskiĭ, ''Regular and chaotic motions in satellite orientation problem,'' preprint No. 53, M. V. Keldysh Institute of Applied Mathematics, Academy of Sciences USSR, 1990.
[24] V. V. Beletskiĭ and A. N. Shlyakhtin, ''Extremal properties of resonance motions,'' Dokl. Akad. Nauk **203**, No. 1 (1972) [Sov. Phys. Dokl. **17**, No. 1 (1972/73)].
[25] G. M. Zaslavskiĭ, R. Z. Sagdeev, D. A. Usikov, and A. A. Chernikov, *Weak Chaos and Quasiregular Structures* (Nauka, Moscow, 1991).
[26] D. V. Pankova, ''On the problem of resonance rotation of a celestial body in the gravitational field of two centers,'' Vestn. Mosk. Univ. Mat. Mekh. No. **4**, 97 (1992).
[27] R. L. Carpenter, ''Study of Venus by CW radar—1964 results,'' Astron. J. **71**, 142 (1966).
[28] V. V. Beletskiĭ, E. M. Levin, and D. Yu. Pogorelov, ''On the question of the resonance rotation of Venus,'' Astron. Zh. **57**, 158 (1980) [Sov. Astron. **24**, 94 (1980)].
[29] V. V. Beletskiĭ, E. M. Levin, and D. Yu. Pogorelov, ''On the question of the resonance rotation of Venus II,'' Astron. Zh. **58**, 198 (1981) [Sov. Astron. **25**, 110 (1981)].
[30] B. G. Bills, W. S. Kiefer, and R. L. Jones, ''Venus gravity: A harmonic analysis,'' J. Geophys. Res. **92**, No. B10, 10 335 (1987).
[31] I. I. Schapiro, D. B. Campbell, and W. M. DeCampli, ''Nonresonance rotation of Venus?,'' Astrophys. J. Lett. **230**, L123 (1979).
[32] A. A. Khentov, ''Formation dynamics of resonance rotations of natural celestial bodies,'' Astron. Zh. **59**, 769 (1982) [Sov. Astron. **26**, 468 (1982)].
[33] A. A. Khentov, ''On the question of interpreting the observed rotation of Venus,'' Astron. Zh. **66**, 202 (1989) [Sov. Astron. **33**, 105 (1989)].
[34] S. J. Peale, ''Some unsolved problems in evolutionary dynamics in the Solar system,'' Celest. Mech. **46**, 253 (1989).
[35] V. V. Beletskiĭ, M. L. Pivovarov, and E. L. Starostin, ''Regular and chaotic motions in the rotation problem of a celestial body in the gravitational field of two centers,'' preprint No. 128, M. V. Keldysh Institute of Applied Mathematics, Academy of Sciences USSR, 1990.
[36] V. V. Beletskiĭ and E. L. Starostin, ''Regular and chaotic rotations of satellite in light flux,'' preprint No. 68, M. V. Keldysh Institute of Applied Mathematics, Academy of Sciences USSR, 1991.
[37] V. V. Beletsky and E. L. Starostin, ''Regular and chaotic rotations of a satellite in sunlight flux,'' in *Nonlinearity and Chaos in Engineering Dynamics*, edited by J. M. T. Thomson and S. R. Bishop (Wiley, New York, 1994).
[38] V. V. Beletsky, *Reguläre und Chaotische Bewegung Sturrer Körper* (Teubner-Verlag, Stuttgart, 1995).